ELSEVIER

Journal of Computational and Applied Mathematics 103 (1999) 125–137

JOURNAL OF COMPUTATIONAL AND APPLIED MATHEMATICS

Numerical grids used in a coastal ocean model with breaking wave effects

Le Ngoc Ly[a,*], Phu Luong[b]

[a] *Department of Oceanography, Naval Postgraduate School, Monterey, CA 93943-5122, USA*
[b] *Stennis Space Center, MS 39529, USA*

Received 28 August 1997; received in revised form 9 February 1998

Abstract

In coastal ocean modeling, traditional single-block rectangular (Cartesian) grids have been most commonly used for their simplicity. In many cases, these grids may be not well suited (even at very high resolutions) for regions with complicated physical fields, open boundaries, coastlines, and bottom bathymetry. The numerical curvilinear nearly orthogonal/orthogonal, single/multi-block coastline-following grids for the Mediterranean Sea, Monterey Bay and the South China Sea (SCS) are presented. These grids can be used in coastal ocean modeling to enhance model numerical solutions and save computer resources by giving better treatment of regions with high gradients such as areas of complicated coastlines and steep slopes of shelf breaks, complicated bottom topography, open boundaries, and multi-scale physical phenomenon. Grid generation techniques are used to designed these grids. This kind of grids can also easily increase horizontal resolutions in the subregion of the model domain, without increasing the computational expense, with a higher resolution over the entire domain.

A three dimensional coastal ocean model with breaking wave effects is also presented and applied. The ocean system is a primitive equation modeling system with grid generation routines and a turbulent closure which is capable of taking surface breaking wave effects into account. The system also includes a grid package which allows model numerical grids to be coupled with the ocean model. The model code is written for multi-block grids, but a single-block grid is used for the South China Sea (SCS). The model with breaking wave effects and a grid of 121×121 grid points are used to simulate the winter circulation of the SCS as an example. The model output of the 60-day run shows the observed upwelling locations in the sea surface salinity field.

Keywords: Numerical grid generation; Nearly orthogonal grids; Multi-block grids; Grids in ocean modeling; Coastal ocean system; Ocean circulation modeling; Breaking wave effects; Mathematical modeling

1. Introduction

It is well known that the solution of a ocean numerical model is strongly dependent on the grid used [7, 12–14]. A not well-suited grid may lead to unsatisfactory ocean model results [12].

* Corresponding author. E-mail: lely@nps.navy.mil.

0377-0427/99/$ - see front matter
PII: S0377-0427(98)00246-5

An improper choice of grid point location can lead to instability or lack of convergence. It is well known that the accurate representation of multi-scale physical phenomena in numerical models has long been a main concern in computational fluid dynamics. One of main concerns of ocean modelers is the capturing of development, evolution, and interaction of various scales of physical phenomena from the small scale of turbulent dissipation to mesoscale eddies, fronts, and larger-scale flows. In this case, with limited computer resources, an appropriate choice of the numerical grid plays a key role in determining the quality of the numerical solution of a coastal ocean model [12, 14].

Rectangular (Cartesian) single-block grids have traditionally used in coastal ocean modeling for their simplicity. However, these grids are unable to handle effectively the solution of problems over arbitrarily shaped complex geometries. Complicated configurations, coastlines, and bottom topographies of oceans and semi-enclosed seas are not well handled by traditional rectangular grids. There are difficulties in interpolations between the boundaries and the interior grid points. This interpolation may produce large errors in the vicinity of strong curvature and sharp discontinuities in oceanic regions with complicated coastlines and bathymetries [7].

Coordinate transformations and mapping the irregular region into a regular one in the computational domain is not new. The technique proposed in [22] reduces a lot of difficulties. Using this technique, transformation is obtained automatically from the solution of some partial differential equations on the regular computational domain. This scheme combines the geometrical flexibility of the finite element method while maintaining the simplicity of the conventional finite difference technique. The method is also called the boundary-fitted coordinate approach.

In coastal ocean modeling, we need a grid system more powerful than a single-block, uniform traditional rectangular grid. The grids for coastal ocean models must be curvilinear, coastline-following, orthogonal/nearly-orthogonal, and multi-block to enhance model numerical solutions. These grids must give better treatment of coastlines and boundary conditions, multi-scale physical phenomenon, and save computational resources. In the case of multi-block grids, the computer resources are not only more effectively used in comparison with the traditional rectangular grids, but more important, the multi-block grids can be used easily and very effectively in parallel computing. These grids can also easily increase horizontal resolution in the subregion of the model domain without increasing the computer expense with high resolution over the entire domain. This goal could be nearly achieved by a nesting technique (interactive nesting) with more complicated processes dealing with boundary conditions, but would be computationally much more expensive. The passive nesting lacks two-way interaction between coarse and fine resolution regions (see [6, 19]). Another problem related to nesting is the interaction between multiple nested meshes, particularly the tendency for propagating dispersive waves to discontinuously change their speeds upon passing from one mesh to the next and to reflect off the boundaries of each nest [6, 19]. This problem is a big concern of nesting technique.

To design the above grids, we need to use a numerical grid generation technique (NGGT). The NGGT is quite popular in engineering flow modeling (see [22]) and lately, the NGGT is used in atmospheric flow modeling [2], but it is still new in coastal ocean modeling. In this study, we apply the NGGT to generate curvilinear orthogonal and nearly orthogonal coastline-following, single-block and multi-block numerical grids for various regions of the world oceans. These grids are to be coupled to a numerical coastal ocean circulation model with breaking wave effects.

2. Grid generation technique and numerical grids used

2.1. Grid generation technique in coastal ocean modeling

The numerical solutions of a coastal ocean model require a discrete set of grid points covering the physical domain (PD). The key issue of grid generation is the mapping the grid points from the PD with x, y and z coordinates to the computational domain (CD) with η, σ, and ζ coordinates. In this study, we focus on 2-D horizontal grid generation. The numerical grid generation and mapping technique of Thompson et al. [21] (the boundary fitted coordinated method) is different from the conventional mapping in that the coordinate transformation relations are defined automatically from the solution of a set of partial differential equation (PDE). The elliptic PDE are frequently used to generate grids. Grids generated from some elliptic systems also generally tend to be smoother than those from algebraic systems.

The mathematical problem of coordinate transformation is to define the relation between the x, y and ζ, η coordinates in the interior points of the PD and CD. The following Poisson's system over the interior region of the PD describes the basic coordinate transformation between the x, y and ζ, η coordinate systems.

$$\frac{\partial^2 \zeta}{\partial x^2} + \frac{\partial^2 \zeta}{\partial y^2} = N(\zeta, \eta), \qquad \frac{\partial^2 \eta}{\partial x^2} + \frac{\partial^2 \eta}{\partial y^2} = M(\zeta, \eta), \tag{1}$$

where $N(\zeta, \eta)$ and $M(\zeta, \eta)$ are the grid control functions. These functions serve to control the spacing and orientation of the grid lines in regions which have large gradients of the physical phenomena (coastline, shelf-break, ocean front regions and regions with steep topography such as sea mounts, submarine canyons). The boundary conditions for solving this system are determined from the fact that the values of ζ and η are specified at every boundary segment of the PD. The above system becomes the Laplace's system if $N = M = 0$.

The Laplace or Poisson type system are the most common form of the elliptic grid generation system, which have smoothing properties and their solutions do not propagate the boundary shape discontinuity into the coordinate field. These systems are more suitable to coastal ocean modeling as they have inherent qualities of smoothness, orthogonality, and good distribution in the interior. Numerical simulations of the coastal ocean model PDE are needed to be performed in the ζ, η coordinates of the CD since the transformed region has simple regular geometry. After that, it is needed to find the (x, y) values of the PD with the known (ζ, η) grid location of the CD. Once the relationship between x, y and ζ, η coordinate values are known at each grid point in the CD, the result can be transformed to the PD. In coastal ocean modeling, the values of the x, y coordinates on the boundaries (coastlines) of the PD are known. They are longitude and latitude values of grid points along the coastlines. And the grid generation problem in coastal ocean modeling becomes one of solving the elliptic grid generation systems over the regular CD with the prescribed values of x, y (longitude and latitude) along the coastlines.

2.2. Numerical grids used for a coastal ocean model

The curvilinear orthogonal and nearly orthogonal coastline-following single-block and multi-block grids are generated for the Mediterranean Sea (MED), Monterey Bay (MOB), and the South China

Sea (SCS) using the EAGLEView grid package [18]. These grids are shown in Figs. 1, 2 and 3, respectively. The rectangular single-block traditional grids are also generated to compare with the curvilinear coastline-following grids. The EAGLEView is a grid generation software that reduces time on the surface definition and refinement process for the solution of the computational field [18]. The EAGLEView implements a grid generation technique by using elliptic, parabolic, hyperbolic, and algebraic generation systems [22]. This package is used as a tool for construction of 2-D and 3-D structured and unstructured surface geometries, and block-structured and unstructured volume meshes. EAGLEView allows the user to define geometry, compute the volume grid, visualize the results, and make changes if necessary without having to execute a different program. The MED coastlines with an eight-block curvilinear nearly orthogonal (8BCNO) coastline-following grid, a single-block traditional rectangular (SBTR) grid, and a nine-block orthogonal (9BO) grid are presented in Fig. 1. The 9BO (lower) and SBTR (middle) grids are designed to have the same horizontal resolution. Even though, the 9BO has 64% of "useful" grid points (MED water grid points) from the total of 17 038 grid points, while the SBTR grid has only 10 953 "useful" grid points from the total of 24 934 grid points (44%). The 9BO grid is 20% more effective in computing resources (storage and CPU time) than the SBTR grid. It is noted that even with this horizontal resolution of 18.38 km $\times$ 13.82 km (supercomputers CRAY-YMP can handle for a primitive equation ocean model with a full turbulence closure and 20–30 vertical levels), the Straits of Gibraltar has two gridlines at most. In this case, the MED is treated as a closed sea without any water exchange with Atlantic ocean. The coastline-following 8BCNO (upper) grid is more powerful than the two above grid for MED.

The three-dimensional view of a SBTR grid (upper) and a single-block curvilinear nearly orthogonal (SBCNO) coastline-following grid (lower) for Monterey Bay (MOB) are presented in Fig. 2. The two grids have the same number of grid points (131×131). The MOB does not have complex coastlines, but it is one region, which has most complicated bottom topography in the world ocean. The SBCNO grid is designed with a high grid density packed along the MOB submarine canyon and steep slopes of shelf break region where topography gradients are large. This SBCNO grid points reduces 40% of the horizontal pressure gradient errors of the MOB ocean model in comparison with the SBTR grid [12]. The SBCNO grid is critically important to the MOB modeling because the SBTR grid model can not handle the MOB complicated bottom topography without losing basic topographic features from the smoothing process. The SBTR grid model accumulates large truncation errors and the model will blow up sometime in the integration process.

Fig. 3 shows the SBTR (left) and SBCNO (right) grids for the South China Sea (SCS) of 121×121 grid points. With the same number of grid points for both grids, the SBCNO has an average horizontal resolution of 12.5×12.5 km, while the SBTR grid has the lower horizontal resolution of 20×20 km. The SBCNO has also better grid densities at the open boundaries which are very important for the SCS ocean modeling.

Overall, the numerical curvilinear nearly orthogonal (also orthogonal multi-block grid) multi and single-block coastline-following grids are used to enhance model numerical solutions by better capturing coastlines, complicated bottom topography and multi-scale physical fields. These grids can also easily increase horizontal resolution in the subregion of the model domain without increasing the computational expense (storage and CPU time) with a higher resolution over the entire model domain.

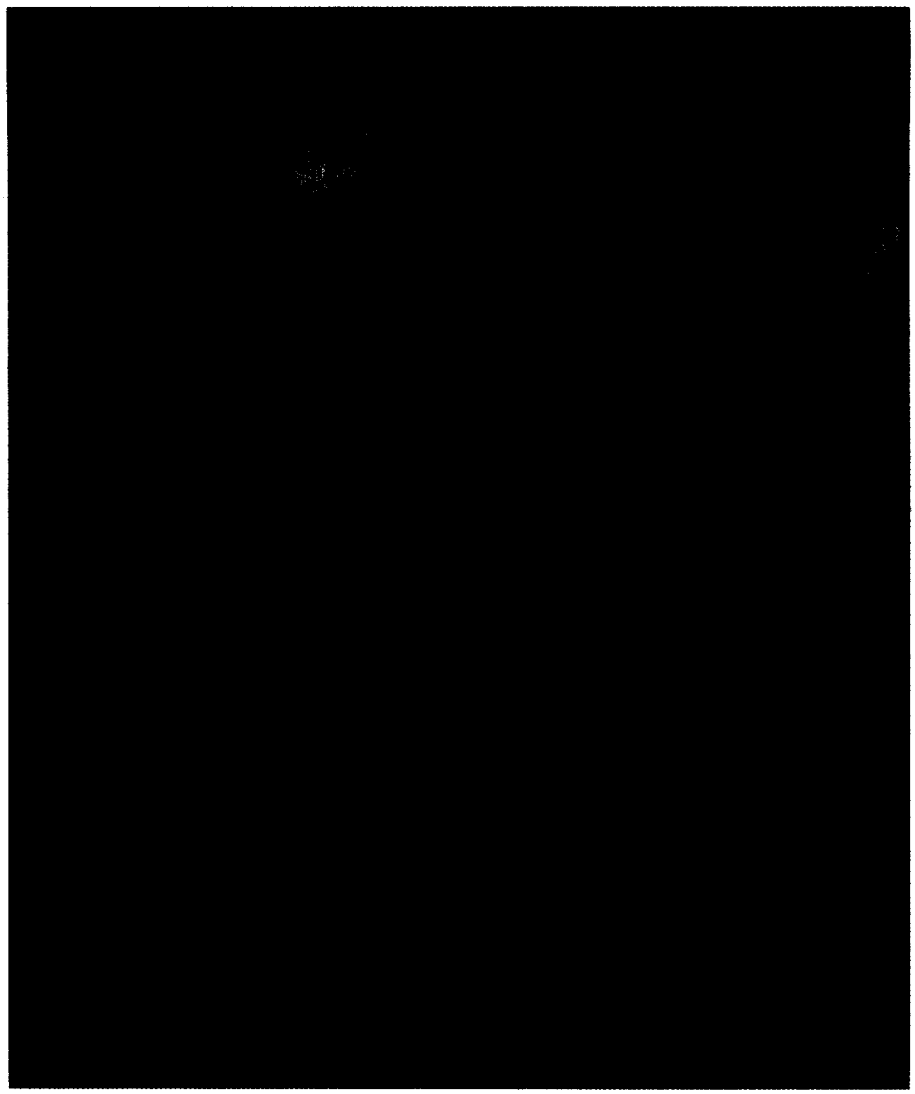

Fig. 1. The Mediterranean Sea coastlines with a curvilinear nearly orthogonal eight-block grid (upper), a traditional rectangular single-block grid (middle), and orthogonal nine-block grid (lower).

3. The model with breaking wave effects and a simulation example

3.1. The model

The model is a three-dimensional primitive equation model which describes the velocity, surface elevation, salinity, and temperature fields in the ocean. The ocean is assumed to be hydrostatic and incompressible (Boussinesq approximation). The equations are written in a system of Cartesian coordinates with x eastward, y northward, and z upward. The motions induced by small-scale processes

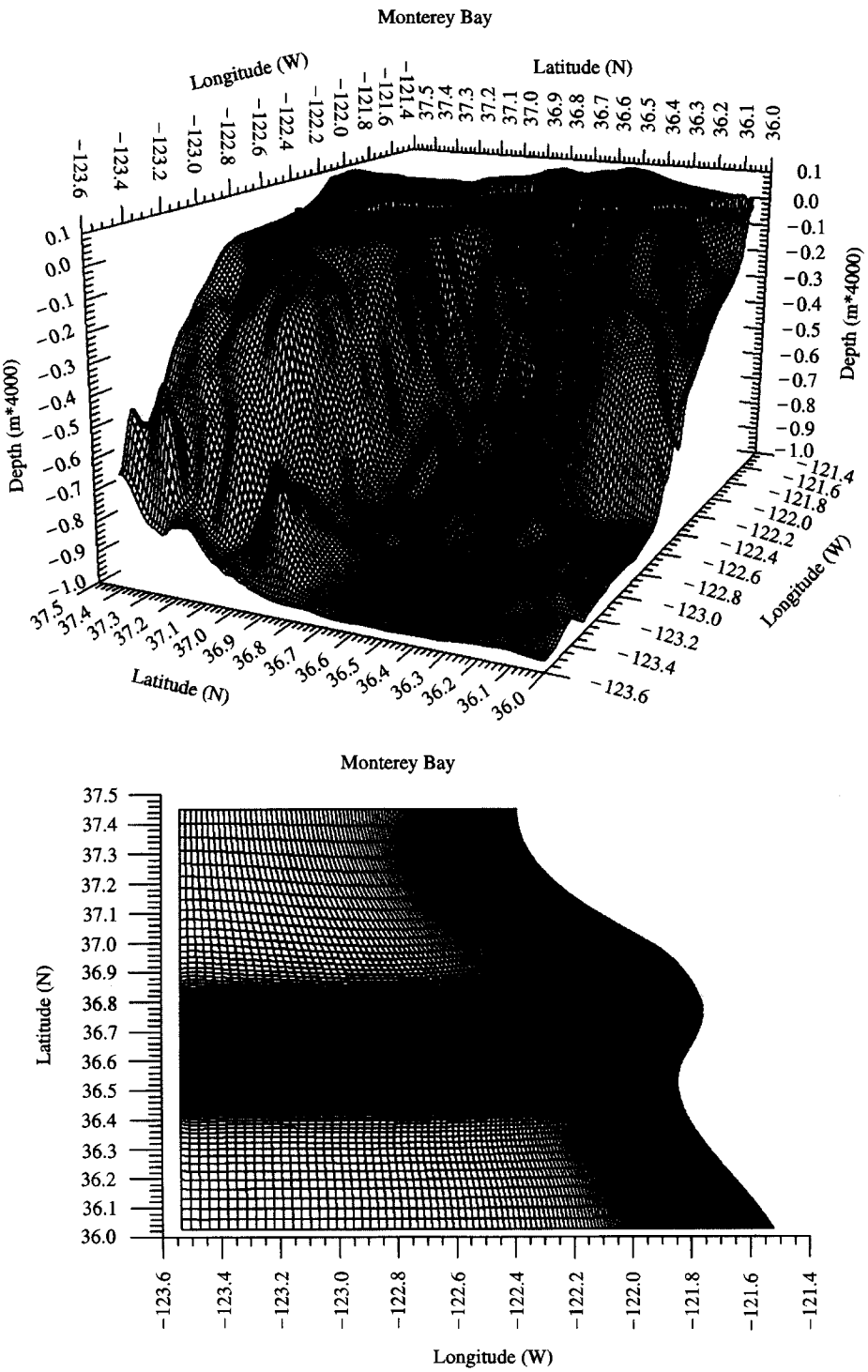

Fig. 2. The 3-D view of a traditional rectangular grid (upper) and a curvilinear nearly orthogonal single-block grid for Monterey Bay.

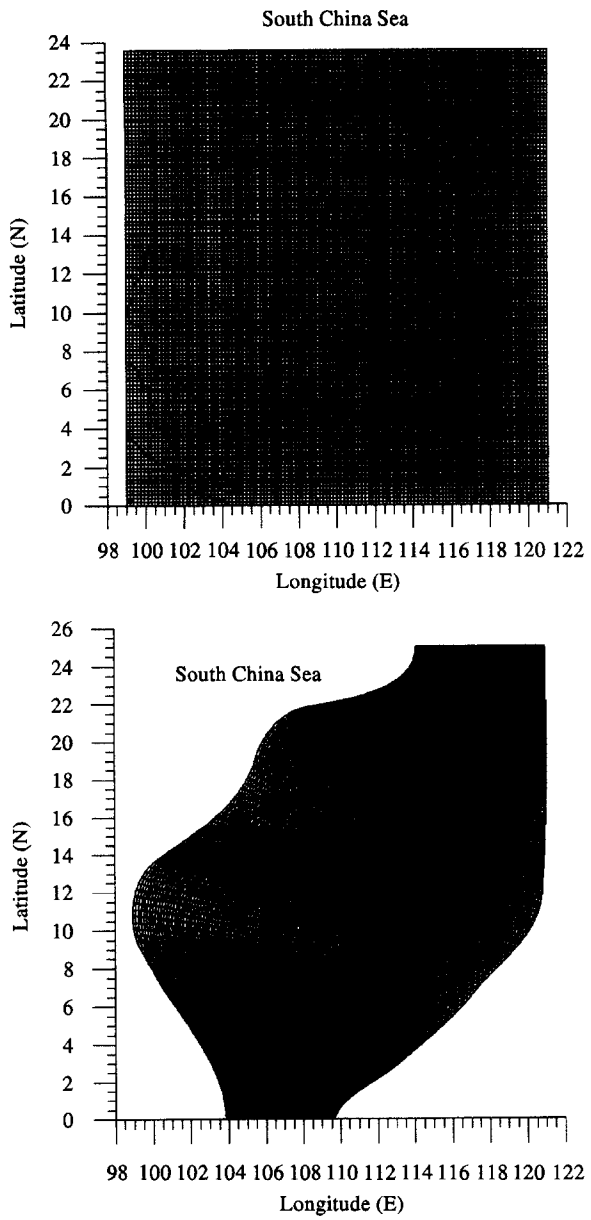

Fig. 3. The South China Sea coastlines with a traditional grid (upper) and a curvilinear nearly orthogonal single-block grid (lower).

not directly resolved by the model grid (subgrid scale) can be parameterized in terms of horizontal mixing processes. These horizontal diffusive terms are for parameterization of subgrid scale processes, but in practice these horizontal diffusive terms are usually required to damp small-scale computational noise [1].

The momentum conservation and diffusion equations contain the vertical turbulent exchange coefficients (TEC) which are determined by the turbulence closure scheme with surface breaking wave effects [9, 10]. This turbulence scheme is characterized by equations for turbulent kinetic energy (TKE), E, for the turbulent dissipation, ε, for the TEC, $K_{m,e,\varepsilon}$, and for parameterization of surface breaking wave effects. Details about the basic model can be found in [15]. The equation for TKE is written in the following form:

$$\frac{\partial E}{\partial t} + \boldsymbol{U}\cdot\nabla E + W\frac{\partial E}{\partial z} = \alpha_1 K_m\left[\left(\frac{\partial U}{\partial z}\right)^2 + \left(\frac{\partial V}{\partial z}\right)^2 - \frac{\alpha_3}{\alpha_1}\frac{g}{\rho_0}\frac{\partial \rho}{\partial z}\right] + \alpha_4\frac{\partial}{\partial z}\left(K_m\frac{\partial E}{\partial z}\right) - \alpha_2\frac{E^2}{K_m} + F_e. \tag{2}$$

The ε-equation is written in a form

$$\frac{\partial \varepsilon}{\partial t} + \boldsymbol{U}\cdot\nabla \varepsilon + W\frac{\partial \varepsilon}{\partial z} = \beta_1 K_m\left[\left(\frac{\partial U}{\partial z}\right)^2 + \left(\frac{\partial V}{\partial z}\right)^2 - \frac{\beta_3}{\beta_1}\frac{g}{\rho_0}\frac{\partial \rho}{\partial z}\right] + \beta_4\frac{\partial}{\partial z}\left(K_m\frac{\partial \varepsilon}{\partial z}\right) - \beta_2\frac{\varepsilon^2}{E} + F_\varepsilon. \tag{3}$$

F_e and F_ε in Eqs. (2) and (3) are the horizontal mixing terms. The TEC for momentum can be calculated using TKE and energy dissipation by the Kolmogorov equation

$$K_m = \alpha_{e\varepsilon}E^2/\varepsilon, \tag{4}$$

where $\alpha_{e\varepsilon} = \alpha_2 = 0.046$ is an universal coefficient [16]. The constants α and β link the TEC for buoyancy and transport with the TEC for momentum [9]

$$\begin{aligned} K_h &= \alpha_3 K_m, \qquad K_{\varepsilon h} = \beta_3 K_m, \\ K_e &= \alpha_4 K_m, \qquad K_\varepsilon = \beta_4 K_m. \end{aligned} \tag{5}$$

Here, the constants α and β have the following values [9]:

$$\alpha_1 = 1.0, \quad \alpha_2 = 0.046, \quad \alpha_3 = 1.0, \quad \alpha_4 = 0.73$$

and

$$\beta_1 = 1.43, \quad \beta_2 = 1.97, \quad \beta_3 = 1.45, \quad \beta_4 = 0.73.$$

These α and β are close to those used in [5] for the ocean mixed layer. A general discussion of the constants is given in [20].

Following Ly [11], the aerodynamic roughness length as seen from above (AR from above, air side AR of the interface), z_{0a}, taking breaking wave effects into account, is assumed to be a function of friction velocities, gravity acceleration, air and seawater densities, and wave age. Based on dimensional analysis, the AR can be written as

$$z_{0a} = a\left(\frac{\rho_a}{\rho}\right)\frac{u_{*a}^3}{g u_p}, \tag{6}$$

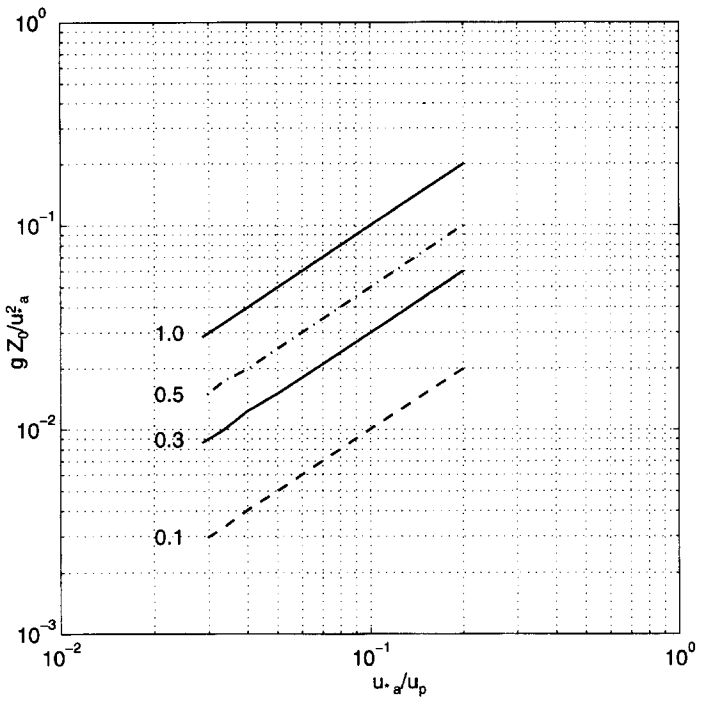

Fig. 4. Non dimensional roughness length from above in dependence on inverse wave age. The lines with numbers are air-wave-sea coupled model outputs with different coefficients in Eq. (6).

where the function $a(\rho_a/\rho)$ may be taken as an empirical constant [8]. Smith et al. [17] used their HEXOS data set and found the empirical constant equal to 0.48. Fig. 4 shows air–wave–sea coupled model z_{0a} in dependence on wave ages. Donelan et al. [3] show that observed data of z_{0a} are very scattered. It may because of the observations were made under various sea status. Ly [11] shows that, in general, the line with coefficient of 0.3 (Fig. 4) is best represented for observed data of various sources which are adapted from [3]. In this model, we use the empirical constant $a(\rho_a/\rho) = 0.30$. Then, our wave-dependent AR length from above has a form

$$z_{0a} = 0.30\frac{u_{*a}^3}{gu_p}. \tag{7}$$

The AR from below (seawater side AR of the interface) can be written as [11]

$$z_{0a} = 28r_l z_0. \tag{8}$$

In this model, we use $r_l = 1/28$, which give $z_{0a} = z_0$. More details about the AR from above and below can be seen in [11].

At the free surface, $z = \eta(x, y)$, the wind stress, heat, and salinity fluxes are prescribed. At the bottom $z = -H(x, y)$, we use zero heat and salinity fluxes conditions. At lateral boundaries the condition of no diffusive fluxes of any property across the interface is used.

The surface boundary condition for TKE is used as follows [10]:

$$E(z)|_{z_0} = \alpha_2^{-1/2} u_*^2, \tag{9}$$

where u_* is the friction velocity of the water flow, and α_2 is a constant as in (2). The continuity condition for momentum fluxes at the air–sea interface can be written as [10]

$$u_* = (\rho_a/\rho)^{1/2} u_{*a} \tag{10}$$

where the subscript "a" is for atmospheric variables.

3.2. Ocean breaking wave effects

Surface ocean wave breaking is considered as an important source of turbulent energy besides the shear driven turbulent energy. Wave breaking has an important role in enhancing turbulence in the upper ocean layer in releasing TKE. The turbulent energy dissipation ε at the air-sea interface can be written in the form [10]

$$\varepsilon(z)|_{z_0} = \frac{u_*^3}{kz_0}[q_1 + (1 - q_1)\exp(-q_2)] + \gamma \frac{u_p^3}{\lambda}\left(\frac{h}{\lambda}\right)^3 \tag{11}$$

where

$$q_1 = \beta_1/\beta_2, \qquad q_2 = (\alpha_2^{1/2}\beta_2/k^2\beta_4)^{1/2}. \tag{12}$$

Here von Karman's constant is assumed to be $k = 0.40$. The first term on the right-hand side of (11) is the dissipation from the mean flow field, and the second term is the dissipation from the surface wave breaking; γ is a nondimensional constant, u_p is wave phase speed, λ and h are wavelength and height, respectively.

The dissipation at the interface can be expressed in terms of the friction velocity, u_{*a}, using a wave breaking condition of the linear theory as follows [10]:

$$\varepsilon(z)|_{z_0} = g u_{*a}\left(\frac{\rho_a}{\rho}\right)^{1/2} \frac{1}{kz_0}[q_1 + (1 - q_1)\exp(-q_{2s})] + \frac{2\gamma c_w}{(2\pi)^4}, \tag{13}$$

where c_w is wave age.

3.3. A simulation example

The Arakawa-C staggered grid [4] and finite difference methods [1] are used to solve the governing equations and boundary conditions. To demonstrate a numerical simulation of the model with a numerical grid, the model is run for the South China Sea (SCS) winter season. The curvilinear nearly orthogonal grid (Fig. 3, right) with 121×121 grid points is used for the SCS model with 16 vertical sigma levels. Here, we have set $q_1 = 1$ and $\gamma = 0$ (without breaking wave effects) to simplify the numerical simulation process. The external (barotropic) mode time step is 30 s, and the internal (baroclinic) mode time step is 15 mins, so that the Courant–Friedrichs–Levy (CFL) computational stability criterion is satisfied. The model is spun up for 30 days and run for 60 days. Fig. 5 shows

Fig. 5. Sea surface salinity field produced by 60-day run for the 16-level South China Sea model with the curvilinear nearly orthogonal single-block grid of 121 × 121 grid points.

the surface salinity field of the 60-day SCS model run. The simulation are computed on the CRAY-YMP supercomputers at the Stennis Space Center and Naval Postgraduate School. At the 60-day the model reproduces a surface salinity field which shows the upwelling locations off the central and southeast Vietnam coast and off the west coast of the Phillippines. These upwelling regions have a high surface salinity greater than 33.9 psu (Fig. 5) and a low temperature of 24.0°C [15] in comparison with their surrounding regions. The locations of the upwelling regions were observed [23].

4. Summary and conclusions

Traditionally, rectangular (Cartesian) single-block grids have been most commonly used in ocean modeling for their simplicity. In many cases, the traditional grids may be not well suited (even at very high resolutions) for regions with complicated physical fields, open boundaries, coastlines, and bottom bathymetry. Here, we present the numerical curvilinear nearly orthogonal, coastline-following single/multi-block grids which can be used in coastal ocean modeling to enhance model numerical solutions for the Mediterranean Sea, Monterey Bay and the South China Sea (SCS) by better treating coastlines, shelf break areas, and regions with complicated bottom topography, open boundaries, and multi-scale physical phenomenon. This kind of grids can also easily increase horizontal resolution in the subregion of the model domain, without increasing the computational expense, with a higher resolution over the entire domain. The grids are designed by using the grid generation technique.

A three-dimensional ocean model with breaking wave effects is also presented and applied. Our coastal ocean system is a primitive equation ocean modeling system with grid generation routines and a turbulent closure which is capable of taking surface breaking wave effects into account. The system also includes a grid package which allows model numerical grids to be coupled with the coastal ocean model. The model code is written for multi-block grids, but a single-block grid is used for the South China Sea (SCS). The coastal ocean model with breaking wave effects and a grid of 121×121 grid points are used to simulate the winter circulation of the SCS as an example. The sea surface salinity field of the model 60-day run shows the observed upwelling locations.

Acknowledgements

The support of the Office of Naval Research under grants N0001498WR30095 and N0001495WR30021 is gratefully acknowledged.

References

[1] A.F. Blumberg, G.L. Mellor, A description of a three-dimensional coastal ocean circulation model, in: Three-Dimensional Coastal Ocean Models, Coastal and Estuarine Sciences, vol. 4, AGU, Washington, DC, 1987, pp. 1–39.

[2] G.S. Dietachmayer, K.K. Droegemeier, Application of continuous dynamic grid adoption techniques to meteorological modeling. Part I: basic formulation and accuracy, Monthly Weather Rev. 120 (1992) 1675.

[3] M.A. Donelan, F.W. Dobson, S.D. Smith, R.J. Andersion, On the dependence of sea surface roughness on wave development, J. Phys. Oceanogr. 6 (1993) 2143.

[4] J.G. Haltiner, R.T. Williams, Numerical Prediction and Dynamical Meteorology, 2nd ed., Wiley, New York, 1980, p. 477.

[5] K.P. Kundu, A numerical investigation of mixed-layer dynamics, J. Phys. Oceanogr. 10 (1980) 220.

[6] M. Laugier, P. Angot, L. Mortier, Nested grid methods for an ocean model: a comparative study, Int. J. Numer. Meth. Fluids 23 (1996) 1163.

[7] P. Luong, L.N. Ly, On an application of multi-block grid technique in coastal ocean modeling: the Mediterranean simulation, AGU Trans. O42B-9 (45) (1995).

[8] L.N. Ly, Modeling the interaction between atmospheric and oceanic boundary layers, including a surface wave layer, J. Phys. Oceanogr. 16 (1986) 1430.

[9] L.N. Ly, An application of the E–ε turbulence model to studying coupled air–sea boundary layer structure, Boundary-Layer Meteorol. 54 (1991) 327–346.

[10] L.N. Ly, A numerical coupled model for studying air-sea-wave interaction, Phys. Fluids 7 (10) (1995) 2396.
[11] L.N. Ly, R.W. Garwood, A numerical study of aerodynamic wave-depended roughness (1999) to be submitted.
[12] L.N. Ly, L. Jiang, Horizontal pressure gradient errors of the Monterey Bay sigma coordinate ocean model with various grids, J. Oceanogr. (1999) in press.
[13] L.N. Ly, P. Luong, Application of grid generation technique in coastal ocean modeling for the Mediterranean, Amer. Geophysical Union (AGU) Trans. 74 (1993) 325.
[14] L.N. Ly, P. Luong, Application of grid generation technique to the Yellow Sea simulation, in: High Performance Computing and Communication (HPC-ASIA 1995), Electronic Proc., CD-ROM, Taipei, Taiwan, 1995.
[15] L.N. Ly, P. Luong, A mathematical coastal ocean circulation system with breaking waves and numerical grid generation, Appl. Math. Modelling 10 (1997) 633.
[16] A.S. Monin, A.M. Yaglom, Statistical Fluid Mechanics: Mechanisms of Turbulence, MIT Press, Cambridge, 1971, p. 769.
[17] S.D. Smith, R.J. Anderson, W.A. Oost, C. Kraan, N. Maat, J. DeCosmo, K.B. Katsaros, K.L. Davidson, K. Bumke, L. Hasse, H.M. Chadwick, Sea surface wind stress and drag coefficients: The HEXOS results, Boundary-Layer Meteorol. 60 (1992) 109.
[18] B.K. Soni, J.F. Thompson, M. Stokes, M.S. Shih, GENIE++, EAGLEView, and TIGER: generation and special purpose graphically interactive grid systems, AIAA 92-0071, 1992.
[19] M.A. Spall, W.R. Holland, A nested primitive equation model for oceanic applications, J. Phys. Oceanogr. 21 (1991) 205.
[20] G. Therry, J. Andre, R. Debar, The energy dissipation function for turbulence closure theory, Phys. Fluids 30(3) (1987) 917.
[21] J.F. Thompson, F.C. Thames, C.W. Mastin, A code for numerical grid generation of boundary-fitted curvilinear coordinated system on fields containing any number of arbitrary two-dimensional bodies, J. Comp. Phys. 24 (1977) 245.
[22] J.F. Thompson, Z.U. Warsi, C.W. Mastin, Numerical Grid Generation: Foundations and Applications, Elsevier, Amsterdam, 1985, p. 483.
[23] K. Wyrtki, Scientific results of marine investigations of the South China Sea and Gulf of Thailand 1959–1961, NAGA Report, vol. 2, 1961.